

A Model for Colour Pattern Formation in the Butterfly Wing of *Papilio dardanus*^a

Toshio Sekimura
College of Engineering, Chubu University
Kasugai, Aichi 487-8501, Japan

Anotida Madzvamuse Andrew J. Wathen
Oxford University Computing Laboratory
Wolfson Building, Parks Road, Oxford OX1 3QD, UK

Philip K. Maini
Centre for Mathematical Biology, Mathematical Institute,
University of Oxford, 24–29 St Giles', Oxford OX1 3LB, UK

The butterfly *Papilio dardanus* is well known for the spectacular phenotypic polymorphism in the female of the species. We show that numerical simulations of a reaction diffusion model on a geometrically accurate wing domain produce spatial patterns that are consistent with many of those observed on the butterfly. Our results suggest that the wing coloration is due to a simple underlying stripe-like pattern of some pigment inducing morphogen. We focus on the effect of key factors such as parameter values for mode selection, threshold values which determine colour, wing shape and boundary conditions. The generality of our approach should allow us to investigate other butterfly species.

Subject classifications: AMS(MOS): 35K55, 65M60, 92-08

Key words and phrases: colour pattern formation, butterfly wing, *Papilio dardanus*, reaction–diffusion equation, Gierer–Meinhardt, finite elements

Oxford University Computing Laboratory
Numerical Analysis Group
Wolfson Building
Parks Road
Oxford, England OX1 3QD

March, 2000

^aAccepted for publication in Proc. Roy. Soc. (Series B).

1 Introduction

There exist very few mathematical models to account for the diversity of colour patterning in butterfly wings. Murray (1981) showed that a diffusing-morphogen-gene-activation system could account for the development of the commonly observed crossbands of pigmentation shortly after pupation. His model was based on the idea of a determination stream proposed by Kühn and von Engelhardt (1933), namely, that the anterior and posterior margins of the wing are sources from which emanate a wave of morphogen concentration. Using a simple diffusion equation, Bard and French (1984) have calculated stable morphogen concentration profiles which simulate the wing pigmentation patterns of three species of butterfly. Based on certain assumptions on morphogen sources and sinks, and morphogen degradation, their results suggest that morphogen gradients can generate some features of butterfly wing patterns. Nijhout (1990) presented a model for colour patterning based on experimental evidence that colour pattern formation is a two-step process: firstly, a spatial distribution of sources and sinks of pattern organizers is set up (during the larval stage); secondly, these organizers induce colour patterning in their surroundings (completed during the late larval and early pupal stages). He showed that the required spatial distribution of sources and sinks could be achieved by signalling determined by the concentration of an activator in a lateral inhibition reaction diffusion model. His model produced patterns consistent with eyespot patterns which are observed along the distal margin of the wing (Nijhout, 1994).

In general, there exist two different kinds of pattern in butterfly wings – colour pattern and the spatial arrangement of scale cells. Colour patterns are formed by the colours of the regularly-arranged scale cells (Sekimura *et al.*, 1998, 1999). The colour of scale cells is mainly due to the presence of chemical pigments, but can sometimes result from diffraction of light in the physically fine-structured scale. The colour patterns of wings are, in general, finely-tiled mosaic patterns produced by overlapping, monochromatic scales and are characteristic of each lepidopteran species (Nijhout, 1991). The timescales on which these two patterns are generated are different from each other. The arrangement pattern of scale cells occurs in the early stages of pupation, while colour patterns appear in the last stage of pupation after completion of cell rearrangement (Nijhout, 1980; Yoshida, 1988). The dimensions of the colour pattern extends from tens to several hundreds of cell diameters, and no cell migration occurs during the period of colour pattern determination. Diffusion of small molecules through gap junctions is assumed to be a feasible mechanism for long distance cell-to-cell communication to form colour patterns (Nijhout, 1991). It is known that the formation of the colour pattern is independent of the arrangement pattern of scale cells, so we assume in our model that colour pattern occurs due to a spatial pattern in pigmentation, not in cell density.

The colour patterns on the wings depend on the species. However, owing to the pioneering work of Schwanwitsch (1924) and Süffert (1927) on the nymphalid ground plan, the complicated colour patterns on butterfly wings can be understood as a composite of a relatively small number of pattern elements. For example, Nijhout (1981) proposed a two-gradient model based on positional information (Wolpert 1969). He hypothesized that the focus of an eyespot was the source of a diffusing chemical (morphogen), the concentration level of which determined the synthesis of certain pigments. This would

only give ring patterns. But the further assumption, that interpretation of the chemical signal depended on cell position (perhaps as the result of a second chemical signal) gave rise to more complicated patterns. These two factors appear to be sufficient to explain thousands of different wing patterns based on the nymphalid ground plan.

More recently, Nijhout (1991) proposed a specific ground plan for *Papilio dardanus*, a species of butterfly widely distributed across sub-Saharan Africa. *Papilio dardanus* is well-known for the spectacular phenotypic polymorphism in females that has evolved as different geographic races have simultaneously come to mimic an array of different species in their specific regions. The females have evolved more than a dozen different wing colour patterns, of which several mimic different species of unpalatable danaids, other butterflies and moths. In addition, females exhibit male-like forms with wing tails in some populations. The males, on the other hand, are monomorphic and strikingly different from the females, exhibiting a characteristic yellow and black colour pattern and tailed hind (Figures 1–4).

According to Nijhout’s idea, there exist four regions – three regions on the forewing and one region on the hindwing – in which (i) the black elements of the colour pattern can increase or decrease in size, and (ii) the background colour of the wing can change independently. The size of the black pattern elements is under independent genetic control. The modifications of the black pattern elements are also quantitative, consisting of variations in the width of existing bands. Widening of black bands constricts the background colour that shows through and can have dramatic effects on the overall appearance of the pattern. The black pattern elements seem to be the main parts of the wing colour patterns, even though the background colour attracts our attention most.

In this paper, we focus on the formation of the black pattern elements on the wing of *Papilio dardanus*. We incorporate two key features of the above models into our reaction diffusion model, namely, the existence of different regions in the wing, and a morphogen interpretation mechanism that is spatially dependent. In Section 2 we briefly describe the reaction diffusion model we use and show some numerical results. Section 3 compares these results with colour patterns observed on the wings of *Papilio dardanus*. The implications of our results are discussed in Section 4.

2 Model and Numerical Results

2.1 Model equations

Since the seminal work of Turing (1952), which showed that a system of reacting and diffusing chemicals could evolve from an initially uniform spatial distribution to concentration profiles that vary spatially – a *spatial pattern* – many models have been proposed exploiting the *short-range activation, long-range inhibition* mechanism used by Turing. One of the earliest models is that of Gierer and Meinhardt (1972). They, in fact, proposed a class of phenomenological models in which the reaction kinetics were chosen to be of activator-inhibitor type. These models all take the general form

$$u_t = f(u, v) + D_1 \nabla^2 u, \quad (2.1)$$

$$v_t = g(u, v) + D_2 \nabla^2 v, \quad (2.2)$$

where $u(\underline{x}, t)$ and $v(\underline{x}, t)$ are chemical concentrations at position \underline{x} and time t , D_1, D_2 are diffusion coefficients and f, g are polynomials or rational functions of u, v which describe the kinetics. These equations are solved on some spatial domain with imposed boundary conditions and initial chemical concentrations are prescribed. These types of model have been analysed in depth mathematically. Using standard linear analysis, conditions can be derived on f, g, D_1 and D_2 under which diffusion-driven instability can arise (see Appendix A). From this analysis, it can be shown that in the vicinity of a primary bifurcation point (where the spatially uniform steady state loses stability) the chemical profiles of u and v are either in phase or 180 degrees out of phase (see, for example, Dillon *et al.*, 1994).

The patterning properties of these models have, in the main, been studied on simple geometrical shapes (for example, rectangles) with zero flux boundary conditions on both species or with both species fixed at the steady state. It is also typically assumed that the domain responds homogeneously to the chemical, that is, there is a spatially uniform threshold level of chemical concentration above which cells differentiate. In this paper, we begin to extend these studies to consider non-standard cases. For the purpose of illustration, we focus on the activator-inhibitor mechanism suggested by Gierer and Meinhardt (1972). This mechanism has been used in a variety of modelling situations (see, for example, Meinhardt, 1982, 1995). The reaction kinetics in the Gierer-Meinhardt model are defined as

$$f(u, v) = k_1 - k_2 u + \frac{k_3 u^2}{v (k_6 + k_7 u^2)}, \quad (2.3)$$

$$g(u, v) = k_4 u^2 - k_5 v, \quad (2.4)$$

where $u(\underline{x}, t)$ and $v(\underline{x}, t)$ are activator and inhibitor concentrations, respectively, at spatial point \underline{x} and time t , and k_1, \dots, k_7 are positive rate constants. The reaction diffusion system can be non-dimensionalised in the standard way (see, for example, Murray, 1993) to yield the system

$$u_t = \gamma \left(a - b u + \frac{u^2}{v (1 + K u^2)} \right) + \nabla^2 u, \quad (2.5)$$

$$v_t = \gamma (u^2 - v) + d \nabla^2 v \quad (2.6)$$

where a, b, d, K and γ are positive parameters, ∇ is the non-dimensionalised spatial operator and, for simplicity, the nondimensionalised chemical concentrations and time are denoted, as before, by u, v and t , respectively.

In the simulations below, we fix the values of $a = 0.1$, $b = 1.0$ and $K = 0.5$, while the values of γ and d are determined from the Turing space according to the mode which would be selected on a unit square domain (see Appendix A). The numerical simulations show the plots of v only. The profiles of u can easily be deduced from these plots as they are in phase with those of v .

2.2 Numerical simulations

We wish to compare our results with the butterfly *Papilio dardanus* so we first trace the forewing and hindwing domains from photographs of the wings of *Papilio dardanus* (Figures 1–2). Then, these shapes are approximated using polygonal domains. The model system is solved on the resulting domain using the finite element method on an unstructured triangular mesh which is generated using a delaunay mesh generator (Müller, Roe & Deconinck, 1993). The numerical simulations are independent of the mesh structure, hence structured or unstructured meshes yield the same numerical solution.

With the kinetic parameters fixed as above, we further select and fix the values $d = 70.8473$ and $\gamma = 619.45$, chosen to select the (3,0) model (see Appendix A) with zero flux boundary conditions on a unit square. Let v_s be the steady state of the concentration v . Assuming that coloration is determined by a constant threshold value in v concentration, v_s say, such that cells in the region where $v \geq v_s$ are black, while cells which experience a concentration $v \leq v_s$, are coloured, these parameters result in a simple pattern of two coloured stripes.

We now allow the threshold function to take the more general form of a plane $\alpha y + \beta x + c_0$ where α or β or both are non-zero and c_0 is a non-negative constant. Here coloration is determined as follows: if cells experience chemical concentration $v \geq \alpha y + \beta x + c_0$ they are black, otherwise they become coloured. By taking this more general form of threshold function, we are making the assumption that the cells within the wing are not necessarily homogeneous in their response to v . Note that if both α and β are zero, then the threshold gradient is reduced to a constant threshold, while if one of α or β is zero, then cells are homogeneous in one direction but have a response gradient in the other direction.

We also allow the boundary conditions to take the more general form

$$\theta (u - u_1) + (1 - \theta) (u_n - u_2) = u_3 \quad (2.7)$$

with a similar form for v , where u_n is the normal derivative at the boundary and we impose values on θ, u_1, u_2 and u_3 . For example, $\theta = 0$ gives a (Neumann) flux condition, while $\theta = 1$ gives a (Dirichlet) fixed condition. Choosing a value of θ between these extremes results in a mixed (Robin) condition. In the simulations below we also allow θ, u_1, u_2 and u_3 to be functions of position along the boundary.

A sample of patterns generated using a threshold function and boundary conditions of the form (2.7) are shown in Figures 5–6 and the parameter values and the boundary conditions used are summarised in Table 1 (Appendix B) and in Figures 7–10 respectively. We shade in white, regions in which the chemical v has concentration less than $\alpha y + \beta x + c_0$, other regions are shaded black.

Although the male and male-like female patterns can be generated using the same model parameters as for the more complicated female patterns, they can also be generated by parameters selected to isolate the (1,0) model on a square domain, with a simple constant threshold value (Figures 11–13). This simpler method of generating male patterns is consistent with the experimental point of view, because these patterns have been genetically considered as the primitive pattern for all other female patterns.

Preliminary numerical simulations suggest that the gross patterning properties of (2.5)–(2.6) are robust to small perturbations of the wing shape for the parameter values

used in this paper. They also suggest that similar results can be produced by different reaction diffusion models. For example, simulations of the Thomas (1975) model and the Schnakenberg (1979) model exhibit similar patterns to those of the Gierer-Meinhardt model.

3 Comparison with *Papilio dardanus*

Comparing Figures 1–4 with our numerical simulations (Figures 5–6) we see that a simple reaction diffusion model can capture the details of the different patterns. In these simulations, for the threshold function the values of $\alpha = -0.111$ and $\beta = -0.025$ are fixed for the forewing patterns in *niobe*, *salaami*, *hippocoonides*, *planemoides* and *trophonius* while for *natalica* the value $\alpha = -0.0555$ is taken. For the hindwing the same values are taken except that α has positive sign (see Appendix B for full details). We find that, under these conditions, the forewing patterns for *niobe*, *salaami*, *hippocoonides* and *trophonius* are generated with the same boundary conditions and with very small changes in c_0 . However, to obtain other patterns, different boundary conditions are used (see Figure 7–10).

Our numerical simulations reveal that only small changes in threshold are necessary to determine different observed patterns. For example, the forewing patterns of the *niobe*, *salaami*, *hippocoonides* and *trophonius* are obtained from the same boundary conditions and parameter values with less than 0.1% change in the threshold. We also find that the boundary conditions play a crucial role in orientation of pattern. A large number of the wing patterns can be simulated with the same boundary conditions. The forewing pattern of *planemoides* is obtained by simply extending the fixed boundary conditions of the *niobe*. The hindwing appears to admit more simple patterns, consistent with the observations in Figures 1–2. These are simulated with the same model parameter values as used for the forewing. The boundary conditions on the hindwing are shown in Figure 10 and are unchanged throughout the different simulations.

4 Conclusion and Discussion

When a particular species exhibits morphological diversity, a key issue is whether or not such diversity can arise from the modification of a basic ground plan pattern. Using a reaction diffusion model, we have found that a fixed set of parameter values, chosen to generate a striped mode on a square domain, can not only generate striped patterns on a wing-shaped domain, but is also sufficient to generate the variety of patterns observed on the fore- and hindwings of *Papilio dardanus*. This suggests that the wing coloration may be due to underlying stripe-like patterns of some pigment inducing morphogen rather than to more complicated patterns. Our results suggest that different colour patterns (black pattern elements here) in females are similar to each other and they could be generated essentially by a fixed set of kinetic and diffusion parameters in a reaction diffusion system. This result could be important from the genetic point of view because it agrees with the result that most of the different forms of the female are controlled by a single genetic locus (Clarke and Sheppard, 1959, 1960).

In our study, the basic ground plan pattern is modified by assuming a threshold function and that boundary conditions can vary among the different butterflies. There is, at present, no direct evidence to support the former, but it is known that certain cell properties do change with position in the wing. For example, the colour patterns are formed by the colours of the regularly-arranged scale cells in the wing and it is known that the adhesive properties of scale cells change with their position in the wing (Nardi, 1988, 1994; Sekimura *et al.*, 1998, 1999). Therefore it is not unreasonable to assume that their sensitivity to a patterning chemical may also vary depending on wing position.

To obtain the variety of realistic female patterns in numerical simulations, we had to choose different types of boundary conditions, suggesting that the wings are composed of areas with different properties. This is consistent with but simpler than the idea proposed by Nijhout (1991) that there exist four regions within the wing (mentioned in the Introduction). Indeed, there is evidence that there is a source of chemical along the distal margin (Koch and Nijhout, in prep). Our results provide an explanation of background coloration that does not require differential growth in several different regions.

Our model simulates the colour pattern by a reaction diffusion mechanism which acts across the whole wing surface. This is different to the model proposed by Nijhout (1991), which views patterning to occur in discrete modules within the wing. The spatial patterns exhibited by our model are produced by diffusion-driven instability from an initially uniform spatial pattern distribution of chemicals, there are no discrete foci of pattern organisers acting as sources and sinks for local pattern elements (Nijhout, 1990).

From our computational results, we also find a hierarchy in relatedness of patterns by combination of some key factors, for example, *planemoides* is similar to the male-like pattern; *niobe*, *salaami*, *trophonius* and *hippocoonides* are almost in the same group; *ce-nea* is close to *leighi*. Since the above results reflect only the aspect of the black pattern elements without taking account of the background colour, we should include the production mechanism of the background colour for more detailed discussions on the relatedness hierarchy which are interesting from the evolutionary point of view. The generality of our approach should allow us to apply our present theory to a wider class of butterflies and to other problems (e.g. evolution of wing colour patterns).

In this paper, we have simulated wing colour patterns of *Papilio dardanus* on adult wing shapes. It is known, however, that the colour patterns are specified earlier during the late larval and early pupal stage when the wing surface is much smaller and different in shape (Nijhout, 1991). Preliminary numerical studies show that the patterns produced by the model mechanism described in this paper are robust to small changes in domain shape and size. A more detailed study of changes in the form of colour pattern during wing development from the larval imaginal disc to the adult wing is of great interest from both theoretical and experimental points of view and it is the subject of further research.

Acknowledgements: TS would like to thank Professor H. F. Nijhout of Duke University for his suggestions and critical reading of the manuscript, and Dr. A. P. Vogler of the Natural History Museum and Imperial College for his critical reading of the manuscript and comments. This work (TS) was in part supported by EPSRC grant (GR/M81878) awarded to M.A.J. Chaplain and PKM, and also by grant from the Human Frontier Science Program (RG0323/1999-M). AM would like to thank the National University of Science and Technology of Zimbabwe for their financial support.

Appendix A: Linear Analysis

Standard linear stability analysis shows that diffusion-driven instability of a steady state of (2.1), (2.2) occurs if the following conditions hold (see, for example, the books by Edelstein-Keshet, 1988; Murray, 1993):

$$f_u + g_v < 0, \quad (4.1)$$

$$f_u g_v - f_v g_u > 0, \quad (4.2)$$

$$df_u + g_v > 0, \quad (4.3)$$

$$(df_u + g_v)^2 - 4d(f_u g_v - f_v g_u) > 0, \quad (4.4)$$

where the partial derivatives are evaluated at the steady state. The inequalities (4.1)–(4.4) define a domain of parameter space, known as the Turing space, wherein the uniform steady state is unstable to small perturbations of given wavenumbers.

Under these conditions, spatial disturbances with wavenumbers $k \in (k_-, k_+)$ will initially grow, where

$$k_{\pm}^2 = \gamma \frac{(df_u + g_v) \pm \sqrt{(df_u + g_v)^2 - 4d(f_u g_v - f_v g_u)}}{2d} \quad (4.5)$$

are the roots of the function on the left-hand side of (4.4). In the case we are interested in, namely, the unit square with zero flux boundary conditions, a further restriction on k is that it must take discrete values $\pi(n^2 + m^2)^{1/2}$, corresponding to the spatial mode $\cos n\pi x \cos m\pi y$ denoted by (n, m) .

For the Gierer-Meinhardt system (2.5) and (2.6) under zero flux boundary conditions, the steady states satisfy

$$f(u, v) = a - bu + \frac{u^2}{v(1 + Ku^2)} = 0, \quad (4.6)$$

$$g(u, v) = u^2 - v = 0. \quad (4.7)$$

To be specific, we fix the values $a = 0.1$, $b = 1.0$ and $K = 0.5$. For these parameters, we solve the steady state equations numerically using the Newton–Raphson method yielding the steady state $(0.8395, 0.7047)$ correct to 6 decimal places.

We wish to isolate a certain mode, that is, we want linear analysis to predict that the uniform steady state goes unstable only to spatial perturbations $\cos n\pi x \cos m\pi y$ with a particular (n, m) . For these parameter values, (4.1) and (4.2) are satisfied, so we need to choose values of d and γ such that (4.3) and (4.4) hold and the (n, m) mode is isolated. By carefully spanning the $d - \gamma$ parameter space we find that the $(3, 0)$ mode can be

isolated for (d, γ) values in a neighbourhood of the point $(70.85, 619.45)$, while the $(1, 0)$ mode can be isolated for values in the neighbourhood of the point $(520.16, 67.00)$.

It should be noted that one could choose different values for a, b and K to satisfy (4.1) – (4.2) and then use the above procedure to determine values of d and γ to isolate mode $(3, 0)$. This would give rise to the same pattern.

We used a similar method to the above to determine parameter values to isolate mode $(3, 0)$ for the Thomas and Schakenberg models. It is important to note that models that take the general form (2.1-2.2) can give rise to similar spatial patterns due to diffusion-driven instability. There are only two major differences: (i) for some models u and v are in phase, in others they are in anti-phase; (ii) some models preferentially exhibit stripes, others exhibit spots – the nature of the pattern is determined by the nonlinearities in the kinetics, with quadratic nonlinearities selecting spots, while cubic nonlinearities will select stripes (Ermentrout, 1990; Nagorcka and Mooney, 1992; Barrio, *et. al.*, 1999).

Appendix B: Parameter Values

Pattern	Forewing	Hindwing
<i>Niobe</i>	$d = 70.8473, \gamma = 619.45$ $\alpha = -0.111, \beta = -0.025, c_0 = 0.69$	Same as forewing except $\alpha = 0.111, \beta = -0.025$ $c_0 = 0.9$
<i>Salaami</i>	Same as for <i>Niobe</i> except $c_0 = 0.695$	$c_0 = 0.89$
<i>Trophonius</i>	Same as for <i>Niobe</i> except $c_0 = 0.697$	$c_0 = 0.91$
<i>Hippocoonides</i>	Same as for <i>Niobe</i> except $c_0 = 0.701$	$c_0 = 0.87$
<i>Planemoides</i>	Same as for <i>Niobe</i> with $c_0 = 0.67$,	$c_0 = 0.7$
<i>Natalica</i>	Same as for <i>Niobe</i> except $\alpha = -0.0555, c_0 = 0.673$	$c_0 = 0.75$
<i>Cenea</i>	Same as <i>Niobe</i> except $\alpha = -0.0111, \beta = -0.025, c_0 = 0.653$	$c_0 = 0.6$
<i>Leighi</i>	Same as <i>Cenea</i> except $c_0 = 0.656$	$c_0 = 0.8$
Male and Male-like	Same as <i>Cenea</i> except $c_0 = 0.95$	$c_0 = 0.75$

Table 1: Table showing parameter values and gradient thresholds used in the numerical simulations.

References

- [1] Bard, J.B.L., & French, V. (1984). Butterfly wing patterns: how good a determining mechanism is the simple diffusion of a single morphogen?, *J. Embryol. exp. Morph.*, **84**, 255-274.
- [2] Barrio, R.A., Varea, C., Aragón, J.L. & Maini, P.K. (1999). A two-dimensional numerical study of spatial pattern formation in interacting Turing systems, *Bull. Math. Biol.*, **61**, 483-505.
- [3] Clarke, C.A. & Sheppard, P.M. (1959). The genetics of some mimetic forms of *Papilio dardanus*, Brown, and *Papilio dardanus*, Linn. *Journal of Genetics*, **56**, 237-259.
- [4] Clarke, C.A. & Sheppard, P.M. (1960). The evolution of mimicry in the butterfly *Papilio dardanus*. *Heredity*, **14**, 163-173.
- [5] Dillon, R., Maini, P.K. & Othmer, H.G. (1994) Pattern formation in generalised Turing systems: I. Steady-state patterns in systems with mixed boundary conditions, *J. Math. Biol.*, **32**, 345-393.
- [6] Edelstein-Keshet, L.(1988). Mathematical Models in Biology, Random House, New York.
- [7] Ermentrout, B. (1990). Stripes or spots? Nonlinear effects in bifurcation of reaction-diffusion equations on the square, *Proc. R. Soc. Lond.*, **A 434**, 413-417.
- [8] Geirer, A. & Meinhardt, H. (1972). A theory of biological pattern formation. *Kybernetik*, **12**, 30-39.
- [9] Kühn, A. & von Engelhardt, A. (1933). Über die determination des symmetriesystems auf dem vorderflügel von *Ephestia kühniella*. *Wilhelm Roux Arch. EntwMech, Org.*, **130**, 660-703.
- [10] Meinhardt, H. (1982). Models of biological pattern formation, Academic Press, New York.
- [11] Meinhardt, H. (1995). The algorithmic beauty of sea shells, Springer-Verlag.
- [12] Müller, J.D., Roe, P.L. & Deconinck, H.(1993). A Frontal Approach for Internal Node Generation for Delaunay Triangulations, *Int. J. of Num. Meth. in Fluids*, Vol. 17, No. **3**, pp 241-56, 1993.
- [13] Murray, J.D. (1981). On pattern formation mechanisms for lepidopteran wing patterns and mamalian coat markings, *Phil. Trans. R. Soc. Lond.*, **B 295**, 473-496.
- [14] Murray, J.D. (1993). Mathematical Biology, Springer-Verlag.
- [15] Nagorcka, B.N. & Mooney, J.R. (1992). From stripes to spots: Prepatterns which can be produced in the skin by a reaction-diffusion system, *IMA J. Math. Appl. Med. & Biol.*, **9**, 249-269.

- [16] Nardi, J.B. (1988). Establishment of a two-dimensional neural network in an insect wing, *Current Issues in Neural Regeneration Research*, Liss A.R., 127-136.
- [17] Nardi, J.B. (1994). Rearrangement of epithelial cell types in an insect wing monolayer is accompanied by differential expression of a cell surface protein, *Dev. Dynamics*, **199**, 315-325.
- [18] Nijhout, H.F. (1980). Ontogeny of the color pattern on the wings of *Precis coenia* (Lepidoptera: Nymphalidae). *Developmental Biology*, **80**, 275-288.
- [19] Nijhout, H.F. (1981). The color patterns of butterflies and moths. *Scientific American*, **245**, No.4, 104-115.
- [20] Nijhout, H.F. (1990). A comprehensive model for colour pattern formation in butterflies. *Proc. R. Soc. Lond.*, B **239**, 81-113.
- [21] Nijhout, H.F. (1991). The development and evolution of butterfly wing patterns. Smithsonian Institution Press, Washington and London.
- [22] Nijhout, H.F. (1994). Genes on the wing. *Science*, **265**, 44-45.
- [23] Schnakenberg, J. (1979). Simple chemical reaction systems with limit cycle behavior. *J. Theor. Biol.*, **81**, 389-400.
- [24] Schwanwitsch, B.N. (1924). On the ground plan of wing-pattern in nymphalids and certain other families of rhopalocerous Lepidoptera. *Proc. Zool. Soc. Lond.*, ser B **34**, 509-528.
- [25] Sekimura, T., Maini, P.K., Nardi, J.B., Zhu M., and Murray, J.D. (1998). Pattern formation in lepidopteran wings. *Comments Theor. Biol.*, **5**, No.2-4, 69-87.
- [26] Sekimura, T., Zhu, M., Cook, J., Maini, P.K., and Murray, J.D. (1999). Pattern formation of scale cells in lepidoptera by differential origin-dependent cell adhesion. *Bull. Math. Biol.*, **61** (in press).
- [27] Süffert, F. (1927). Zur vergleichende analyse der schmetterlingszeichnung. *Biologisches zentralblatt* **47**, 385-413.
- [28] Thomas, D. (1975). Artificial enzyme membrane, transport, memory, and oscillatory phenomena. in *Analysis and Control of Immobilized Enzyme Systems*, edited by D. Thomas and J.-P. Kervenez. New York: Springer Verlag.
- [29] Turing, A.M. (1952). The chemical basis of morphogenesis, *Phil. Trans. Roy. Soc. Lond.* B**237**, 37-72.
- [30] Wolpert, L. (1969). Positional information and the spatial pattern of cellular differentiation, *J. Theor. Biol.* **25**, 1-47.
- [31] Yoshida, A. (1988). *Spec. Bull. Lep. Soc. Jap.*, **6**, 447. (in Japanese).

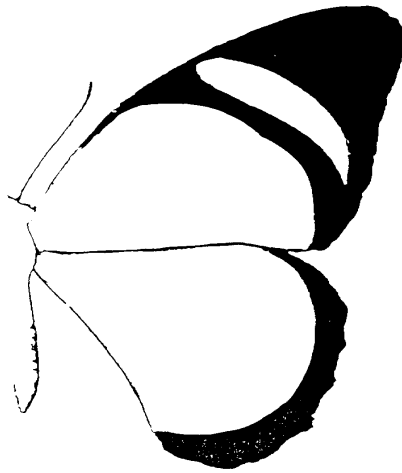


Figure 1: (i) Polymorphism in females of *Papilio dardanus*. (a) *Trophonius*, (b) *cenea*, (c) *planemoides* and (d) *hippocoonides*.



Figure 2: (ii) Male pattern. (courtesy of Drs A. P. Vogler and A. Cieslak of the Natural History Museum, London, and Imperial College, Silwood Park).

Papilio dardanus
(a) mimetic forms



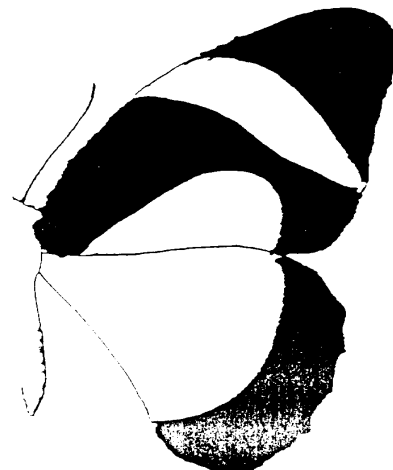
(i) *trophonius*



(ii) *cenea*



(iii) *planemoides*

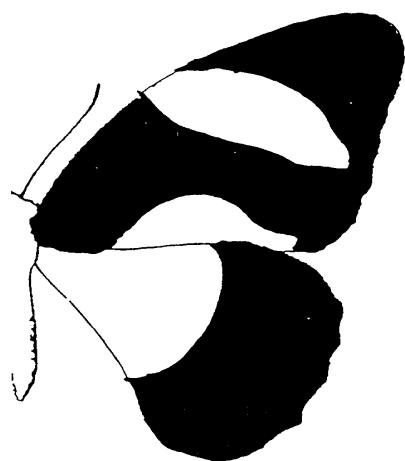


(iv) *hippocooides*

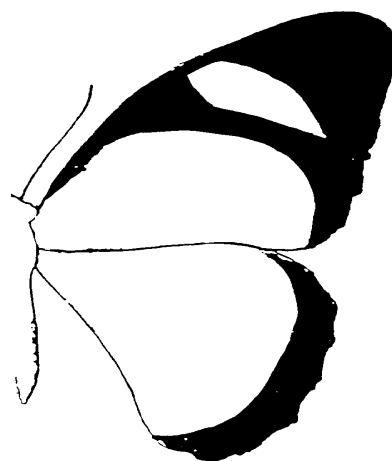
(a) ———

Figure 3: Diagram illustrating the black patterned elements in mimetic and non-mimetic forms of *Papilio dardanus*. (a) Mimetic forms: (i) *trophonius*, (ii) *cenea*, (iii) *planemoides*, (iv) *hippocooides*.

Papilio dardanus
(b) non-mimetic forms



(i) *natalica*



(ii) *niobe*



(iii) *leighi*



(iv) *salaami*

(e)

Figure 4: Figure 3 cont'd: (b) Non-mimetic forms: (i) *natalica*, (ii) *niobe*, (iii) *leighi*, (iv) *salaami*. (with permission of Professor H.F. Nijhout of Duke University).

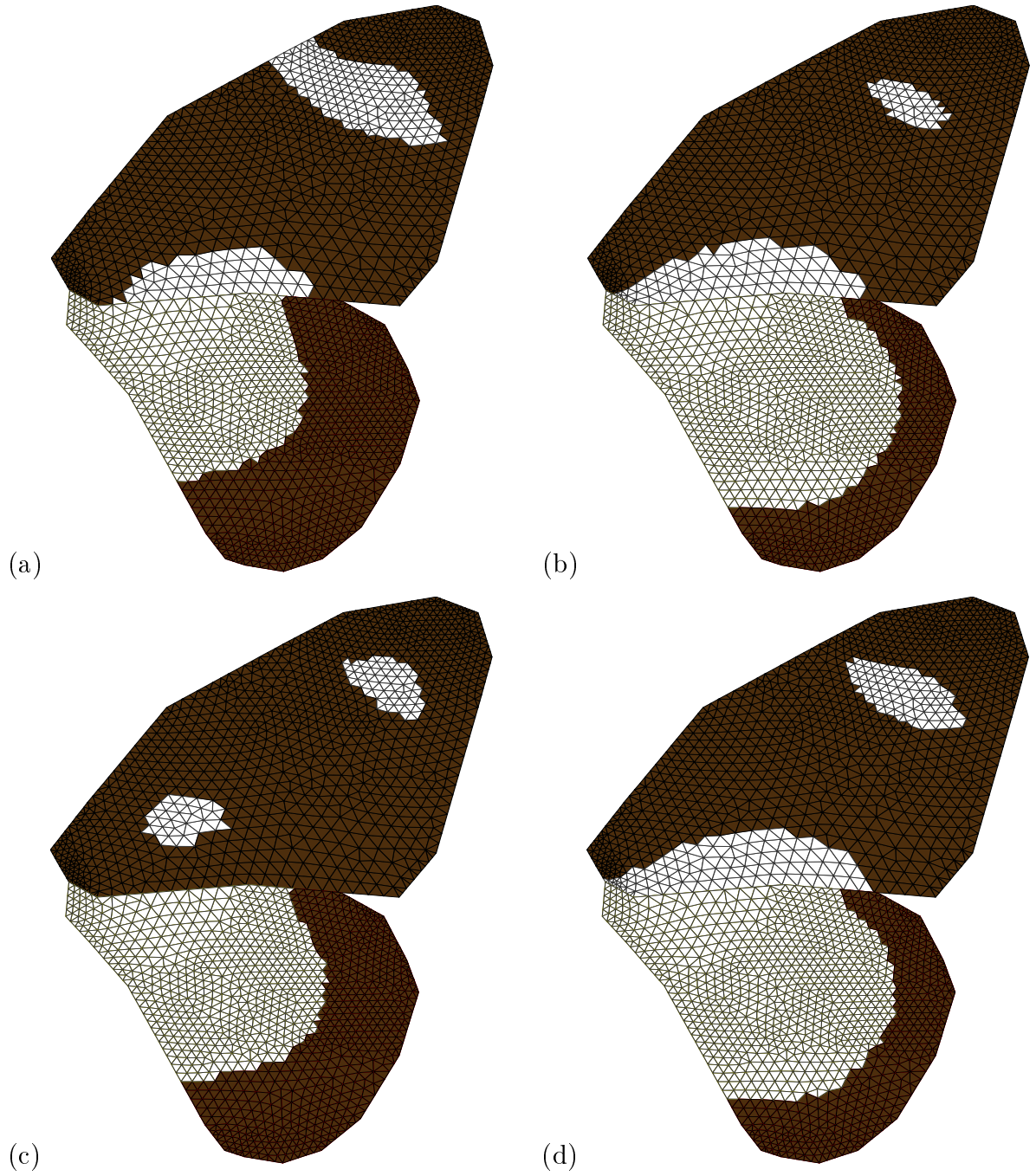


Figure 5: Results of numerical simulations of the Geirer-Meinhardt model (2.5)–(2.6). For comparison with *Papilio dardanus* see Figures 1–4. (i) mimetic forms: (a) *trophonius*, (b) *cenea*, (c) *planemoides*, (d) *hippocoonides*.

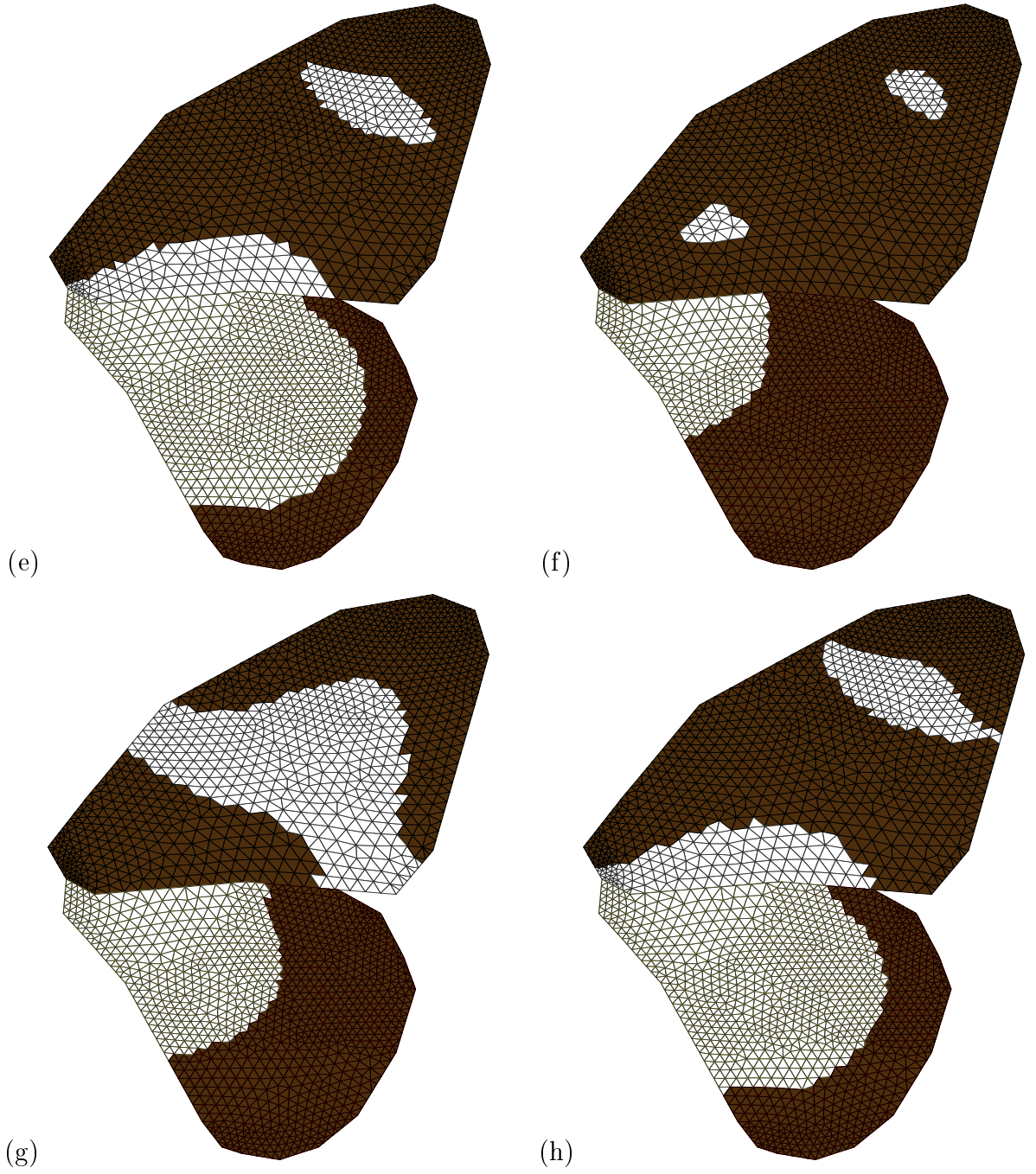


Figure 6: Figure 5 cont'd: (ii) non-mimetic forms: (e) *natalica*, (f) *niobe*, (g) *leighi*, (h) *salaami*. Black indicates concentrations of v above the threshold gradient, white indicates values below the threshold gradient. Model and threshold parameters are given in Appendix B, boundary conditions are shown in Figures 7–10.

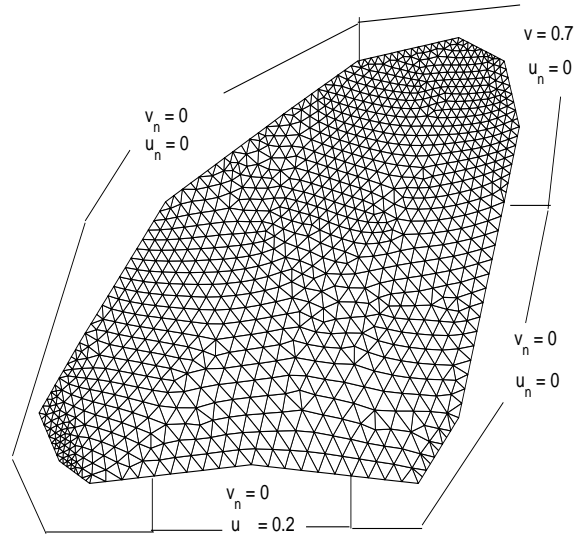


Figure 7: Boundary conditions for the simulations shown in Figures 5–6. (a) Forewings of (i) *natalica*, *niobe*, *salaami*, *trophonius* and *hippocoonides*.

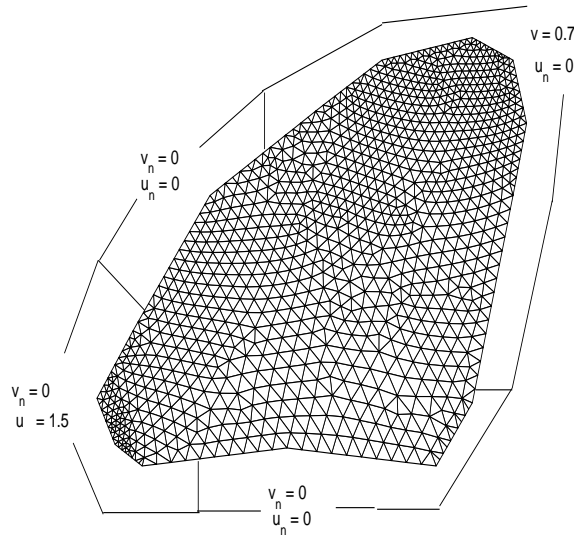


Figure 8: (ii) Boundary conditions to simulate *planemoides*

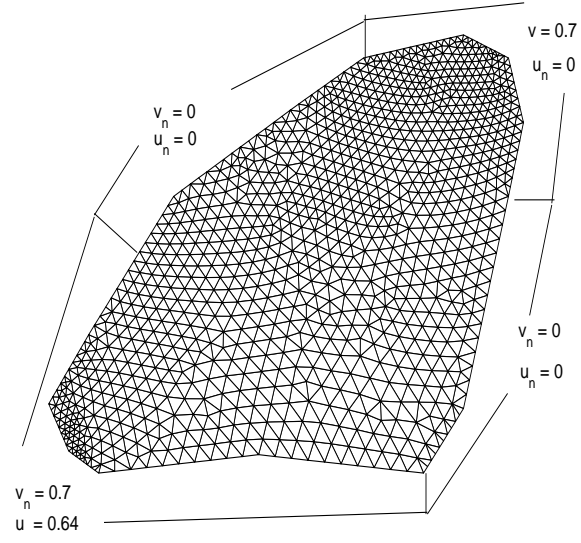


Figure 9: (iii) Corresponding boundary conditions for *cenea* and *leigh*.

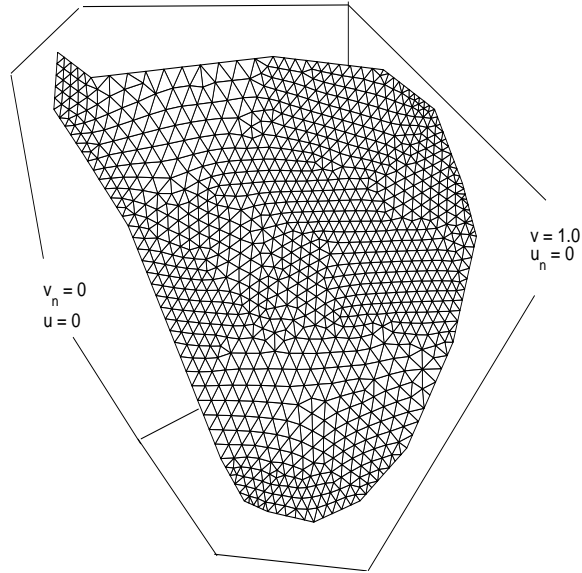


Figure 10: (b) Boundary conditions for the hindwing (all butterflies). These figure also shows the mesh on which the numerical calculations were performed.

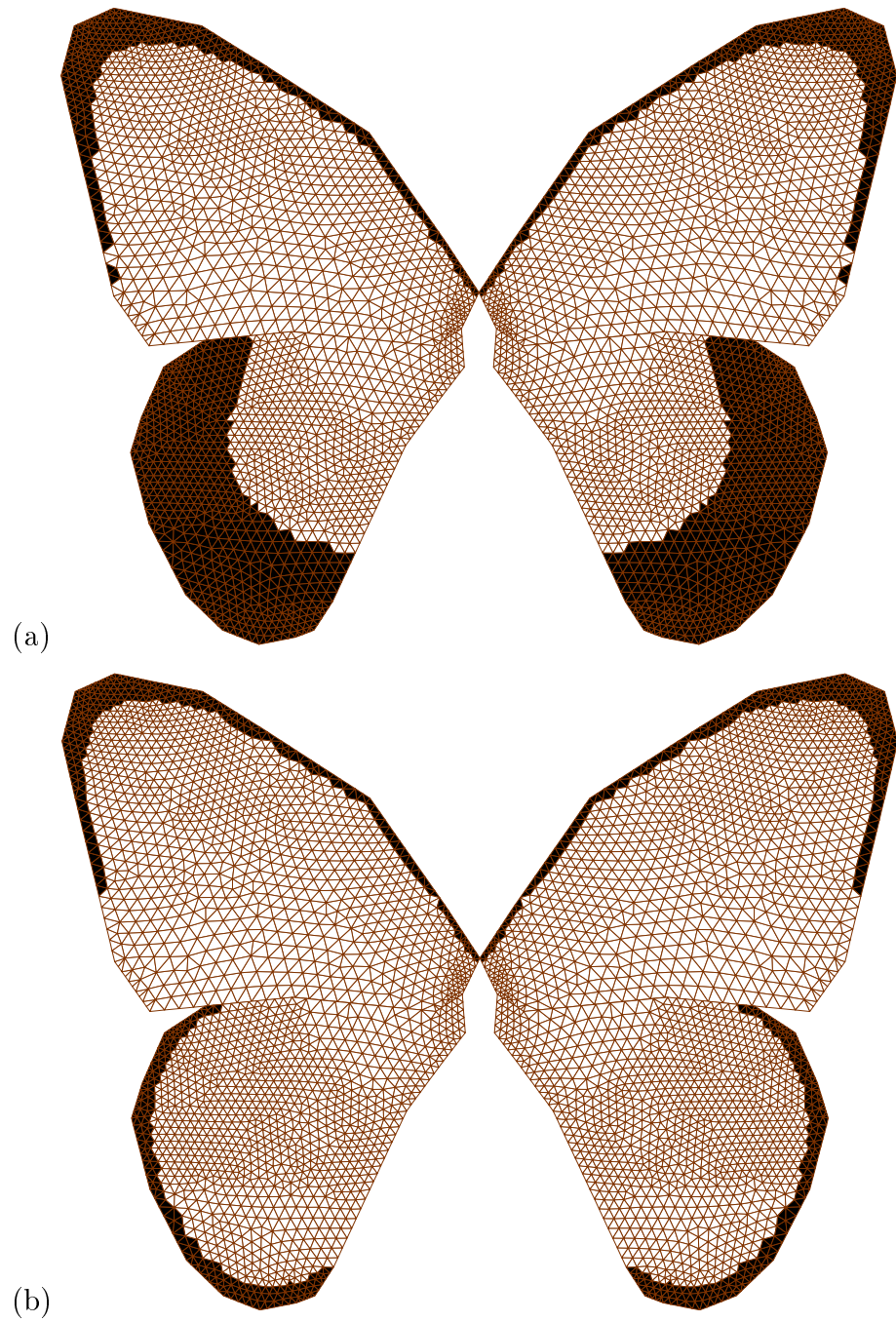


Figure 11: Results of numerical simulations of the Geirer-Meinhardt model (2.5)–(2.6) for the male pattern. (a) Parameters corresponding to the (3,0) mode (see Appendix A); (b) Parameters corresponding to the (1,0) (a , b , K as for the (3,0) mode, but $d = 520.157$, $\gamma = 67$) with a constant threshold value of 0.999 for the forewing and 0.699 for the hindwing.

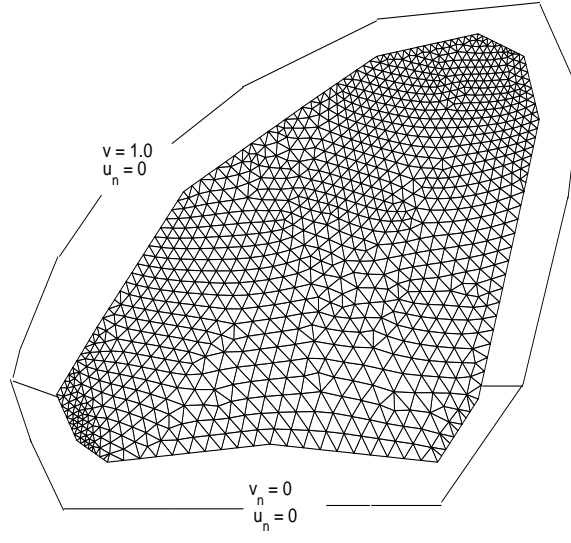


Figure 12: (c) Boundary conditions for the forewing numerical result in Figure 11.

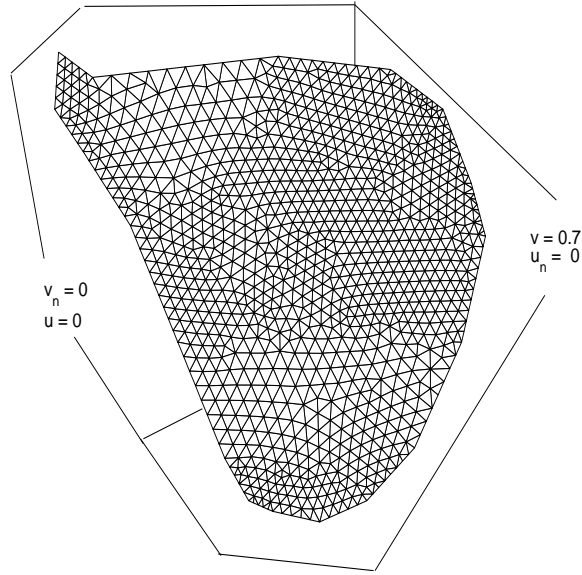


Figure 13: Boundary conditions for the hindwing numerical result in Figure 11.